ELSEVIER

Contents lists available at ScienceDirect

Fitoterapia

journal homepage: www.elsevier.com/locate/fitote





Four unreported aporphine alkaloids with antifungal activities from *Artabotrys hexapetalus*

Pei Zhao a,b,c, Zhiyin Yu a, Jian-Ping Huang b, Li Wang a, Sheng-Xiong Huang a,b,*, Jing Yang b,*

- ^a College of Ethnic Medicine, Chengdu University of Traditional Chinese Medicine, Chengdu, China
- b State Key Laboratory of Phytochemistry and Plant Resources in West China, Kunming Institute of Botany, Chinese Academy of Sciences, Kunming, China
- ^c Yinchuan Hospital of Traditional Chinese Medicine, Yinchuan, China

ARTICLE INFO

Keywords: Artabotrys hexapetalus Aporphine alkaloids Hexapetalusines A-D Antifungal activities

ABSTRACT

In this study, the extract from *Artabotrys hexapetalus* showed strong antifungal activity against phytopathogenic fungi in vitro. Four unreported aporphine alkaloids, hexapetalusine A-D (1–4), were isolated from stems and roots of *Artabotrys hexapetalus* (L.f.) Bhandari, along with six known aporphine alkaloids (5–10). Their chemical structures were elucidated by extensive spectroscopic analysis. The absolute configurations of 1–3 were determined using single-crystal X-ray diffractions and ECD calculations. Hexapetalusine A-C (1–3) were special amidic isomers. Additionally, all isolated compounds were evaluated for their antifungal activity against four phytopathogenic fungi in vitro. Hexapetalusine D (4) exhibited weak antifungal activity against *Curvularia lunata*. Liriodenine (5) displayed significant antifungal activity against *Fusarium proliferatum* and *Fusarium oxysporum* f. sp. *vasinfectum*, which is obviously better than positive control nystatin, suggesting that it had great potential to be developed into an effective and eco-friendly fungicide.

1. Introduction

Plant-infecting fungi have been jeopardizing food security world-wide through infection calorie and commodity crops [1], leading to substantial crop yield losses of about 20% worldwide [2]. Furthermore, the extensive use of antifungal agents in agriculture has resulted in selection for resistance in the fields that make it more difficult to combat fungal pathogens [3]. Therefore, there is a growing need to discover and develop new fungicides derived from natural products to effectively safeguard crops [4].

In the continuation of our antifungal activity against phytopathogenic fungi screenings of the extracts libraries from plants and endophytes in special ecological niches [5,6], the extract of stems and roots of *Artabotrys hexapetalus* (L.f.) Bhandari displayed significant antifungal activity against phytopathogenic fungi in vitro. *A. hexapetalus* is a traditional folk medicinal plant, which is used in Asian to treat microbial infections and other diseases [7]. Various classes of bioactive compounds have been isolated such as aporphine alkaloids [8–10], terpenoids [11,12], flavonoids [13], etc. Among them, aporphine alkaloids have reported to have various activities [14–22]. In this study, four new aporphine alkaloids, including three amidic aporphines (1–3) and an

unusual aporphinoid alkaloid related to telisatin-type aporphinoids (4), together with six previously described aporphines, liriodenine (5) [23], atherospermidine (6) [24,25], artabonatine C (7) [25], norstephalagine (8) [26], lettowianthine (9) [27], and artacinatine (10) [8], were isolated from stems and roots of A. hexapetalus (Fig. 1). In addition, liriodenine (5) displayed broad antifungal activity. Herein, we describe the isolation, structural elucidation and antifungal activity of these compounds.

2. Results and discussion

Compound **1** was acquired as colorless needle crystals and its molecular formula $C_{19}H_{17}NO_5$ was determined by HRESIMS spectrum m/z 340.1179 [M + H] $^+$ (calcd. 340.1179), accounting for 12 degrees of unsaturation. The UV absorption bands of **1** at 205, 219, 241 and 280 nm suggested aporphine alkaloids [28]. 1 H NMR spectrum of **1** was complex, which showed two sets of signals in a ratio of about 7:1. Amidic aporphines, with either *N*-formyl or *N*-acetyl group, always exist as mixture of enolates arising from the restricted amide rotation of two isomers with steric hindrance [29,30], indicating that compound **1** may belong to the class of amidic aporphines. 1 H NMR data of **1** showed a

E-mail addresses: sxhuang@mail.kib.ac.cn (S.-X. Huang), yangjingc@mail.kib.ac.cn (J. Yang).

^{*} Corresponding authors at: State Key Laboratory of Phytochemistry and Plant Resources in West China, Kunming Institute of Botany, Chinese Academy of Sciences, Lanhei Road 132, 650201 Kunming, China.

P. Zhao et al. Fitoterapia 174 (2024) 105868

typical resonance of an *N*-formyl proton at $\delta_{\rm H}$ 8.34 (1H, s, H-13) and a methoxyl group at $\delta_{\rm H}$ 4.05 (3H, s) (Table 1). Two doublets at $\delta_{\rm H}$ 5.99 (d, J=1.4 Hz) and 6.12 (d, J=1.4 Hz) were characteristic signals of a methylenedioxy group [31]. Furthermore, the $^1{\rm H}$ NMR and $^1{\rm H}-^1{\rm H}$ COSY data (Fig. 2) indicated an AA'BB' aromatic system at $\delta_{\rm H}$ 7.39 (1H, d, J=7.5, H-8), 7.28 (1H, td, J=7.5, 1.0, H-9), 7.42 (1H, td, J=7.8, 1.2, H-10), 8.13 (1H, d, J=7.8, H-11) in ring D. The $^{13}{\rm C}$ NMR data in combination with HSQC of 1 suggested the presence of 19 carbons, including a *N*-formyl carbon ($\delta_{\rm C}$ 162.5), two aromatic rings ($\delta_{\rm C}$ 145.2, 140.3, 135.9, 121.7, 121.4, 110.4, 135.3, 129.7, 129.5, 129.4, 127.9 and 127.2), three methylenes ($\delta_{\rm C}$ 24.7, 43.7 and 101.2), two methines ($\delta_{\rm C}$ 53.7 and 70.7) and one methoxy carbon ($\delta_{\rm C}$ 59.8) (Table 2).

These spectra data indicated 1 had similar features to those of known N-formyl-annonain [30]. Further NMR analysis revealed other differences, including the C-3 was replaced by methoxy group supported by the HMBC correlations from $\delta_{\rm H}$ 4.05 (–OCH₃) to $\delta_{\rm C}$ 140.3 (C-3) (Fig. 2), and the C-7 [$\delta_{\rm H}$ 5.02 (1H, d, J=2.6), $\delta_{\rm C}$ 70.7] was oxidized to hydroxyl group. Thus, the planar structure of 1 was assigned and further verified by detailed analysis of its 2D NMR (Fig. 2). The ROESY correlations of H-13 ($\delta_{\rm H}$ 8.34, s) with H-5 β ($\delta_{\rm H}$ 3.90) suggested that the major isomer of 1 was Z configuration. The absolut configuration of 1 was finally determined as 6aS and 7R by using single-crystal X-ray (Table S1, Fig. S1 and Fig. 3) and electronic circular dichroism (ECD) calculations (Tables S2-S3, Fig. S2 and Fig. 4). Accordingly, compound 1 was named as hexapetalusine A.

Compound 2, isolated as a white solid, was deduced to have a molecular formula of $C_{18}H_{15}NO_4$ by HRESIMS m/z 332.0891 [M + Na] (calcd. 332.0893), with 12 degrees of unsaturation. The ¹H NMR spectrum of 2 exhibited two sets of signals, implying that it may be also an amidic aporphine. In the NMR spectrum, two amide conformations were observed in a ratio of approximately 6:1. A careful comparison of the NMR data between 2 and 1 (Tables 1 and 2) revealed that 2 was closely similar to those of 1, except for the absence of a methoxyl group at C-3 ($\delta_{\rm C}$ 109.0) in **2**. This conclusion was further confirmed by the HMBC correlations from H-3 ($\delta_{\rm H}$ 6.68, s) to C-1 ($\delta_{\rm C}$ 144.8), C-2 ($\delta_{\rm C}$ 148.9), C-3a ($\delta_{\rm C}$ 130.5) and C-4 ($\delta_{\rm C}$ 31.8) (Fig. 2). The Z-form isomer of 2 was established based on the NOESY correlation between H-13 ($\delta_{\rm H}$ 8.35) and H-5 β ($\delta_{\rm H}$ 4.01). The absolute configuration of 2, in accordance with those of compound 1, was established on the basis of ECD calculations of (6aS, 7R) using time-dependent density functional theory (TDDFT) (Tables S5-S6 and Fig. S3). The calculated ECD spectrum of 2 was in good agreement with the experimental one (Fig. 4), and named as hexapetalusine B.

Compound 3 was purified as a white solid. The HRESIMS displayed a

Table 1 ¹H NMR data of compounds **1–4** ($\delta_{\rm H}$ in ppm, J in Hz).

Position	1 ^{a,e}	2 b,e	3 ^{c,e}	4 ^d
3		6.68 s		7.12 s
4	2.52 m	2.88 td (15.2,	3.02 brd	3.34 m
	3.09 brd (16.2)	4.0)	(15.8)	
		2.80 brd	2.50 td (15.8,	
		(15.2)	3.6)	
5	3.54 td (12.6, 2.9)	3.55 td (12.3,	3.47 m	3.48 m
	3.90 ddd (12.7,	2.3)	4.06 m	3.66 m
	4.9, 1.5)	4.01 m		
6a	5.14 brs	5.00 brs	5.32 brs	
7	5.02 d (2.6)	4.95 d (2.6)	4.98 d (1.8)	
8	7.39 d (7.5)	7.40 d (7.0)	7.38 d (7.3)	8.53 d (7.9)
9	7.28 td (7.5, 1.0)	7.34 td (7.0,	7.28 t (7.5)	7.51 td (7.9,
		1.2)		0.9)
10	7.42 td (7.8, 1.2)	7.44 td (7.9,	7.41 t (7.6)	7.34 td (8.2,
		1.2)		1.1)
11	8.13 d (7.8)	8.22 d (7.9)	8.13 d (7.9)	8.77 d (8.2)
12	5.99 d (1.4)	6.02 brs	5.98 s	6.30 d (1.3)
	6.12 d (1.4)	6.12 brs	6.12 s	6.31 d (1.3)
13	8.34 s	8.35 s		
14			2.27 s	
15				1.5 s
3 -OCH $_3$	4.05 s		4.05 s	

- ^a Recorded at 600 MHz in CDCl₃.
- ^b Recorded at 600 MHz in CD₃OD.
- c Recorded at 800 MHz in CDCl₃.
- ^d Recorded at 800 MHz in CD₃OD.
- ^e The NMR data are reported for the major rotamer.

signal for $[M + H]^+$ at m/z 354.1339 (calcd. for $C_{20}H_{19}NO_5$, 354.1336), indicating 12 degrees of unsaturation. The UV spectrum of 3 (204, 219, 240, 281 nm) resembled those of 1 (205, 219, 241, 280 nm), suggesting 3 is an analogue of 1. The comparison of the 1D NMR data of compound 3 with those of 1 showed that compounds 3 and 1 were similar apart from N-acylated substitution in 3 replacing N-formylated group in 1 (Tables 1 and 2). Compound 3 was also observed as a pair of rotational isomers with a ratio of approximately 10:1 in the ¹H NMR. Intriguingly, compound 3 was also structurally similar to puberulumine K [31]. The main difference in the structure lied in the configuration of C-7, and this was deduced by comparing the J values between H-6a and H-7, which were found to be 1.8 Hz in 3 and 12.6 Hz in puberulumine K, suggesting that the cis relationship between H-6a and H-7 in 3. Similarly, the ROESY correlation between H-5 β ($\delta_{\rm H}$ 4.06) and H-14 ($\delta_{\rm H}$ 2.27) indicated that the major isomer 3 was Z conformation. As similar ECD spectra curve among compounds 1 and 3 were observed (Fig. 4), the absolute

Fig. 1. Structures of compounds 1-10.

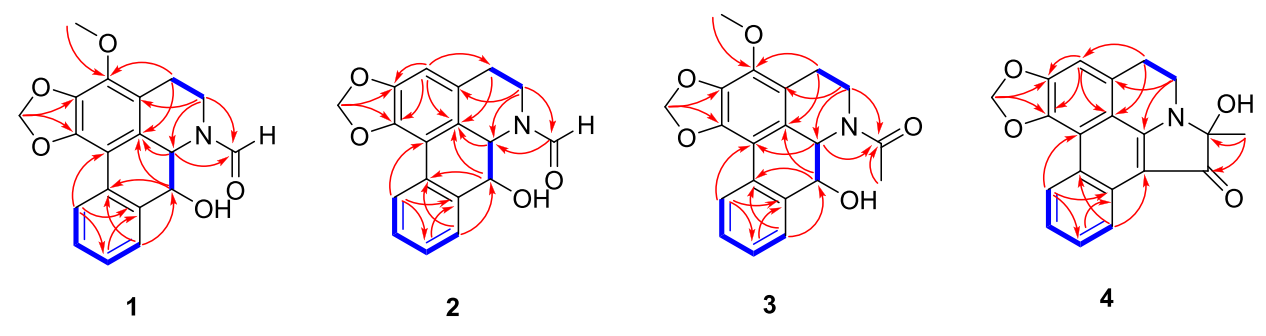


Fig. 2. Key $^{1}H^{-1}H$ COSY (blue lines) and HMBC (red arrows) correlations of compounds 1–4. (For interpretation of the references to colour in this figure legend, the reader is referred to the web version of this article.)

Table 2 ¹³C NMR data of Compounds **1–4** ($\delta_{\rm C}$ in ppm).

Position	1 a,e	2 ^{b,e}	3 ^{c,e}	4 ^d
1	145.2 s	144.8 s	145.0 s	144.0 s
1a	110.4 s	117.2 s	110.5 s	120.7 s
1b	121.4 s	121.6 s	122.7 s	114.9 s
2	135.9 s	148.9 s	135.6 s	152.4 s
3	140.3 s	109.0 d	140.3 s	109.3 d
3a	121.7 s	130.5 s	122.1 s	131.9 s
4	24.7 t	31.8 t	24.6 t	29.3 t
5	43.7 t	45.2 t	43.8 t	38.9 t
6a	53.7 d	55.2 d	54.5 d	163.1 s
7	70.7 d	70.6 d	71.3 d	102.6 s
7a	135.3 s	137.2 s	135.8 s	130.4 s
8	129.4 d	130.4 d	129.4 d	123.6 d
9	127.9 d	129.6 d	127.8 d	129.6 d
10	129.7 d	130.2 d	129.6 d	124.8 d
11	127.2 d	128.7 d	127.1 d	128.7 d
11a	129.5 s	131.1 s	129.4 s	124.9 s
12	101.2 t	102.5 t	101.2 t	103.4 t
13	162.5 d	164.9 d	169.8 s	90.9 s
14			22.8 q	200.1 s
15			•	20.5 q
3-OCH ₃	59.8 q		59.8 q	•

- ^a Recorded at 150 MHz in CDCl₃.
- $^{\rm b}$ Recorded at 150 MHz in CD₃OD.
- $^{\rm c}$ Recorded at 200 MHz in CDCl3.
- ^d Recorded at 200 MHz in CD₃OD.
- ^e The NMR data are reported for the major rotamer.

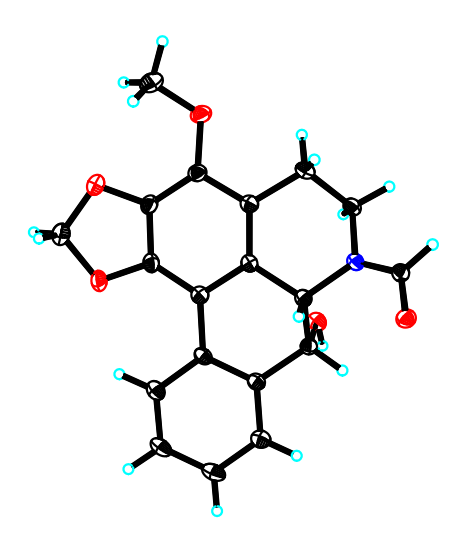


Fig. 3. X-ray molecular structure of 1.

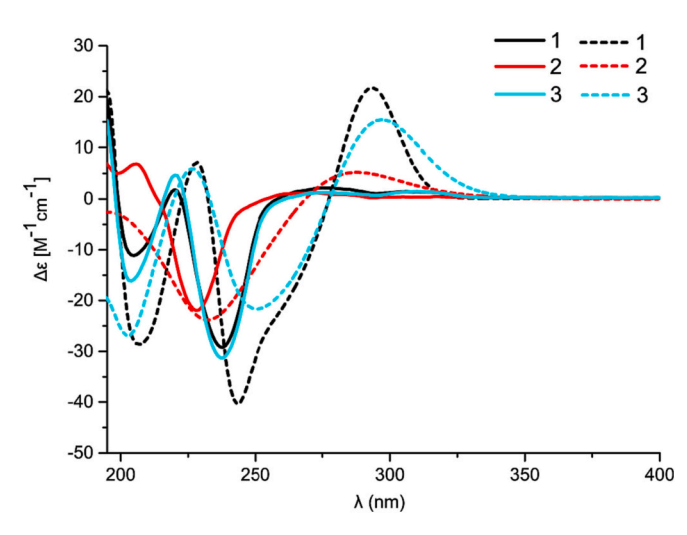


Fig. 4. Experimental (solid lines) and calculated (dotted lines) ECD spectra of compounds 1–3.

configuration of 3 was also identified as 6Z-(6aS, 7R) (Tables S8-S9 and Fig. S4), and named as hexapetalusine C.

Compound 4 was obtained as a yellow solid and ascertained as $C_{20}H_{15}NO_4$ from the HRESIMS spectrum m/z 334.1069 [M + H] + (calcd. 334.1074), accounting for 14 degrees of unsaturation. The ¹H NMR data of the aromatic hydrogen signals at $\delta_{\rm H}$ 8.77 (1H, d, J=8.2 Hz, H-11), 8.53 (1H, d, J = 7.9 Hz, H-8), 7.51 (1H, td, J = 7.9, 0.9 Hz, H-9), and 7.34 (1H, td, J=8.2, 1.1 Hz, H-10) revealed a 1,2-disubstituted benzene (Table 1). The ¹³C and HSQC spectra of 4 suggested the presence of 20 carbons, which were classified into one methyl ($\delta_{\rm C}$ 20.5), one sp³ quaternary carbon (δ_C 90.9), three methylenes (δ_C 103.4, 38.9 and 29.3), nine aromatic nonprotonated carbons ($\delta_{\rm C}$ 163.1, 152.4, 144.0, 131.9, 130.4, 124.9, 120.7, 114.9, 102.6), five aromatic methines ($\delta_{\rm C}$ 129.6, 128.7, 124.8, 123.6 and 109.3), and one carbonyl carbon ($\delta_{\rm C}$ 200.1) (Table 2). ${}^{1}H - {}^{1}H$ COSY correlations of 4 showed two spincoupling systems consisting of H-4/H-5 and H-8/H-9/H-10/H-11 (Fig. 2). The key HMBC correlations from H-3 to C-1/C-2/C-1b, from H-4 to C-3/C-1b, from H-5 to C-6a/C-3a, from H-8 to C-7/C-11a, from H-11 to C-1a/C-7a, and from H-12 to C-1/C-2 further suggested the existence of an aporphine skeleton (Fig. 2). The methyl proton singlet at $\delta_{\rm H}$ 1.5 (3H, s, H₃-15) was assigned as C-15 based on HMBC correlations of H₃-15 with C-13/C-14. Thus, the planar structure of 4 was determined. In addition, compound 4 was an unusual aporphine alkaloid with a methyl group and a hemiaminal structure as a substituent at C-13. To assign the absolute configuration of 4, ECD spectrum was acquired. However, no Cotton effect was observed in ECD spectrum of 4, which inferred that compound 4 seems to be racemate. Thus, compound 4 was named hexapetalusine D.

All the isolated compounds were tested for their antifungal activity

against four phytopathogenic fungi in vitro by the filter paper agar diffusion method [32]. Hexapetalusine D (4) exhibited weak antifungal activity against *Curvularia lunata* (Table 3). Liriodenine (5) displayed significant antifungal activity against *Fusarium oxysporum* f. sp. *vasinfectum* and *Fusarium proliferatum*, which was obviously better than positive control nystatin (Table 3), suggesting that it had great potential to be developed into an effective and eco-friendly fungicide.

Alkaloids, one of the main active components of *A. hexapetalus*, can be divided into benzylisoquinolines, morphanes, protoberberines, aporphines and other classes according to varied scaffolds, in which the number and species of aporphines are abundant. Compounds **1–3** were established as amidic aporphine alkaloids, in which diastereotopic atoms have two chemical shifts detectable by 1D NMR spectroscopy, resulting from restricted N—C (O) bond rotational barrier [33]. Liriodenine (5), a type of representative oxoaporphines, contains planar π^* – π conjugated system in molecular skeleton [34]. We also studied that liriodenine (5) was more active against *F. oxysporum* f. sp. *vasinfectum* and *F. proliferatum* than positive control nystatin, which has not been reported. However, compounds **1–3** failed to inhibit four phytopathogenic fungi in vitro, whether this implied that the amide structure was involved. More experiments are still need to confirm this supposition.

3. Material and methods

3.1. General experimental procedures

MCI gel (CHP20/P120) for column chromatography (CC) was produced by Mitsubishi Chemical Corp., Japan. Silica gel (200-300 mesh) for CC and silica GF254 for Thin-layer chromatography (TLC) were vielded by Qingdao Marine Chemical Inc., China, Sephadex LH-20 was purchased from Pharmacia Biotech Ltd., Sweden. Semipreparative highperformance liquid chromatography (HPLC) was recorded on a Hitachi Chromaster system (Hitachi Ltd., Japan) equipped with a YMC Triart C18 column (250 \times 10 mm i.d., 5 μ m), using a flow rate of 3.0 mL/min at a column temperature of 28 °C, and detection was performed with a DAD detector. HRESIMS spectra were recorded on an Agilent Auto SpecPremier G6230 mass spectrometer. The UV spectra were taken on a Shimadzu UV-2700 spectrophotometer (Shimadzu Corp., Japan). Optical rotation was determined in MeOH on an Autopol VI manufactured by Rudolph Research Analytical, Hackettstown, NJ, USA. CD spectra were measured on an Chirascan V100 Applied Photophysics digital circular dichroism chiroptical spectrometer (Applied Photophysics Limited, Surrey, UK). X-ray crystallographic analysis was carried out with a Bruker APEX DUO singlecrystal X-ray diffractometer (Bruker Corp., Germany). NMR spectra were conducted on a Bruker Avance III 600 or a Bruker Ascend™ 800 (Bruker Corp., Germany), and tetramethylsilane (TMS) was used as internal standard.

3.2. Plant material

The roots and stems of *A. hexapetalus* were collected in August 2020 in Bawangling Botanical Garden, Hainan Province, China, and identified by Prof. Zhigai Guo, Institute of Tropical Bioscience and Biotechnology, Chinese Academy of Tropical Agricultural Sciences. The voucher

Table 3 Antifungal activities of compounds 4 and 5 $^{\rm a}$.

Test fungi	4	5	Nystatin ^b
F. oxysporum f. sp. vasinfectum	0	13.0 ± 0.8	9.7 ± 0.6
F. proliferatum	0	17.0 ± 0.8	6.3 ± 0.6
F. oxysporum	0	6.0 ± 0.8	9.8 ± 0.3
C. lunata	6.3 ± 0.6	14.0 ± 0.8	29.0 ± 1.0

^a Evaluated in inhibition zone diameters (mm) at 10 μ g/disk. Results are expressed as mean \pm SD (n=3).

specimen (No. Hsx-Ah-1 *A. hexapetalus*, Hainan) was preserved at State Key Laboratory of Phytochemistry and Plant Resource in West China, Kunming Institute of Botany, Chinese Academy of Sciences, Kunming, China.

3.3. Extraction and isolation

The air-dried and powdered roots and stems of A. hexapetalus (5.0 kg) were extracted (each 3×24 h) with 95% EtOH at room temperature. The 95% EtOH extract was evaporated to afford a viscous residue (0.5 kg). This extract was subjected to chromatography by Macropore adsorptive resin D101 and eluted with a H2O-MeOH gradient system (8:2, 6:4, 4:6, 2:8, 0:10, each 20 L). The 60% EtOH fraction (158 g) was chromatographed over silica gel CC and eluted with increasing polarities of CHCl2-MeOH (100:0 to 0:100) to yield five factions (A-E). Fraction B was further fractionated by MCI gel (CHP20/P120) in H2O-MeOH to give seven subfractions (B1-B7). Subfraction B6 was applied to Sephadex LH-20 employing MeOH as mobile phase, followed by purification using semipreparative HPLC (45% and 30% MeCN-H2O, v/v, respectively) to yield compounds 1 (1.0 mg), 5 (5.2 mg), and 8 (1.8 mg). Subfractions B5 and B7 were separately rechromatographed over Sephadex LH-20 eluting MeOH, proceeded by preparation with semipreparative HPLC (30% MeCN-H2O, v/v) to obtain compounds 3 (1.5 mg), 4 (1.3 mg), 6 (4.4 mg), 7 (1.2 mg), 9 (1.4 mg) and 10 (1.1 mg). Fraction C was separated using the same procedures as for Fraction B to obtain ten subfractions (C1-C10). Subfraction C10 was resolved by Sephadex LH-20 using a step gradient elution of MeOH combined with semipreparative HPLC (32% MeCN-H2O, v/v) to give compound 2 (1.1 mg).

3.3.1. Hexapetalusine A 1

Colorless needle crystals; $[\alpha]_D^{25}$ –423.0 (c 0.16, MeOH); ECD (MeOH) $\lambda_{\rm max}$ ($\Delta\varepsilon$) 205 (–11.13), 218 (0.65) and 238 (–29.20) nm; UV (MeOH) $\lambda_{\rm max}$ (log ε) 205 (4.53), 219 (4.46), 241 (4.28) and 280 (4.27) nm; 1 H and 13 C NMR data, see Tables 1 and 2; HRESIMS m/z 340.1179 [M + H] $^+$ (calcd. for $C_{19}H_{18}NO_5^+$, 340.1179).

3.3.2. Hexapetalusine B 2

White amorphous solid; $[\alpha]_D^{25}$ –276.4 (c 0.06, MeOH); ECD (MeOH) $\lambda_{\rm max}$ ($\Delta\varepsilon$) 206 (6.79) and 228 (–22.06) nm; UV (MeOH) $\lambda_{\rm max}$ (log ε) 205 (4.39), 273 (4.02) and 280 (3.95) and 319 (3.58) nm; $^1{\rm H}$ and $^{13}{\rm C}$ NMR data, see Tables 1 and 2; HRESIMS m/z 332.0891 [M + Na] $^+$ (calcd. for ${\rm C}_{18}{\rm H}_{15}{\rm NO}_4{\rm Na}^+$, 332.0893).

3.3.3. Hexapetalusine C 3

White amorphous solid; $[a]_{2}^{25}$ -231.7 (c 0.27, MeOH); ECD (MeOH) $\lambda_{\rm max}$ ($\Delta\varepsilon$) 204 (-16.41), 220 (4.46) and 237 (-31.53) nm; UV (MeOH) $\lambda_{\rm max}$ (log ε) 204 (4.17), 219 (4.09), 240 (3.90) and 281 (3.90) nm; $^{1}{\rm H}$ and $^{13}{\rm C}$ NMR data, see Tables 1 and 2; HRESIMS m/z 354.1339 [M + H] $^{+}$ (calcd. for ${\rm C}_{20}{\rm H}_{20}{\rm NO}_{5}^{+}$, 354.1336).

3.3.4. Hexapetalusine D 4

Yellow amorphous solid; $[\alpha]_D^{25}$ 0 (c 0.05, MeOH); UV (MeOH) $\lambda_{\rm max}$ (log ε) 249 (4.39), 257 (4.52) and 282 (4.29) nm; 1 H and 13 C NMR data, see Tables 1 and 2; HRESIMS m/z 334.1069 [M + H] $^+$ (calcd. for $C_{20}H_{16}NO_4^+$, 334.1074).

3.3.5. Crystal data for 1

 $C_{19}H_{17}NO_5$, M=339.33, $\alpha=19.2196$ (5) Å, b=19.2196 (5) Å, c=7.7317 (2) Å, $\alpha=90^\circ$, $\beta=90^\circ$, $\gamma=120^\circ$, V=2473.40 (14) Å3, T=150. (2) K, space group P65, Z=6, μ (Cu K α) = 0.828 mm-1, 27,700 reflections measured, 3023 independent reflections ($R_{int}=0.1712$). The final R_I values were 0.0639 ($I>2\sigma$ (I)). The final wR (F^2) values were 0.1611 ($I>2\sigma$ (I)). The final R_I values were 0.0749 (all data). The final wR (F^2) values were 0.1712 (all data). The goodness of fit on F^2 was

b Positive control.

1.108. Flack parameter = 0.22 (18). Crystallographic data for compound 1 have been deposited in the Cambridge Crystallographic Data Centre (CCDC) with number 2303236. Copies of the data are available from the website of CCDC free of charge.

3.4. Antifungal assay

The antifungal activity of all the isolated compounds were tested in vitro by the filter paper agar diffusion method against Curvularia lunata KIB-C01, Fusarium oxysporum KIB-F01, Fusarium oxysporum f. sp. vasinfectum KIB-F02 and Fusarium proliferatum KIB-F03, as previously described [32]. Curvularia lunata, Fusarium oxysporum, Fusarium oxysporum f. sp. vasinfectum and Fusarium proliferatum were provided by Northeast Agricultural University, Harbin, China and based on their ITS gene sequences, identified with GenBank accession nos. PP260021, PP260000, PP260022 and PP292065, respectively. Initially, all fungi were retrieved from the storage tube and cultured for 2 weeks at 30 °C on potato dextrose agar (PDA). Subsequently, the fungi were incubated in PDA at 30 °C for one week to obtain new mycelium for the antifungal assays. The medium was mixed with the plant pathogenic fungi suspension at about 45 °C, ensuring that the abundance of the strains is about 10⁸ cfu/mL. Autoclaved paper disks with a diameter of 6 mm were placed around the fungal inoculant on the same Petri dish. Each paper disk was impregnated with 10 µg testing samples and nystatin (positive control). Fungal inoculants were cultivated in dark at 30 °C for 2 days, and then the size of the inhibition zones was analyzed by cross bracketing method. All tests were performed in triplicate.

Funding

This research was funded by the National Natural Science Foundation of China (82225043 and 32271480); the "Xinglin Scholar" Research Promotion Project of Chengdu University of TCM (BSH2021034 and BSH2021013); the China Postdoctoral Science Foundation (2022M710497).

CRediT authorship contribution statement

Pei Zhao: Writing – original draft, Investigation, Data curation, Conceptualization. Zhiyin Yu: Writing – review & editing, Writing – original draft, Visualization. Jian-Ping Huang: Writing – review & editing, Writing – original draft, Data curation. Li Wang: Writing – review & editing, Writing – original draft, Data curation. Sheng-Xiong Huang: Project administration, Funding acquisition, Conceptualization. Jing Yang: Writing – review & editing, Visualization, Conceptualization.

Declaration of competing interest

The authors declare that they have no known competing financial interests or personal relationships that could have appeared to influence the work reported in this paper.

Data availability

Data will be made available on request.

Acknowledgments

The authors are grateful to Dr. Xiao-Nian Li at Analysis and Testing Center, Kunming Institute of Botany, Chinese Academy of Sciences for the measurement and analysis of the single-crystal X-ray diffraction data.

Appendix A. Supplementary data

NMR spectra of compounds 1–4, crystal data and structure refinement for 1, X-ray packing diagram of 1, and antifungal assay of tested compounds are available as Supporting Information. Supplementary data to this article can be found online at https://doi.org/10.1016/j.fitote.2024.105868.

References

- [1] M.C. Fisher, S.J. Gurr, C.A. Cuomo, D.S. Blehert, H.L. Jin, E.H. Stukenbrock, J. E. Stajich, R. Kahmann, C. Boone, D.W. Denning, N.A.R. Gow, B.S. Klein, J. W. Kronstad, D.C. Sheppard, J.W. Taylor, G.D. Wright, J. Heitman, A. Casadevall, L.E. Cowen, Threats posed by the fungal kingdom to humans, wildlife, and agriculture, mBio 11 (2020) e00449–20.
- [2] M.C. Fisher, N.J. Hawkins, D. Sanglard, S.J. Gurr, Worldwide emergence of resistance to antifungal drugs challenges human health and food security, Science 360 (2018) 739–742.
- [3] S. Sun, M.J. Hoy, J. Heitman, Fungal pathogens, Curr. Biol. 30 (2020) R1163–R1169.
- [4] Y.B. Bai, M. Zhang, D. Li, Y. Zhao, L.Z. Huang, J.M. Gao, Synthesis and antifungal activity of derivatives of the natural product griseofulvin against phytopathogenic fungi, J. Agric. Food Chem. 71 (2023) 6236–6248.
- [5] C. Liu, L. Bai, P. Cao, S. Li, S.X. Huang, J. Wang, L. Li, J. Zhang, J. Zhao, J. Song, P. Sun, Y. Zhang, H. Zhang, X. Guo, X. Yang, X. Tan, W. Liu, X. Wang, W. Xiang, Novel plant growth regulator guvermectin from plant growth-promoting rhizobacteria boosts biomass and grain yield in rice, J. Agric. Food Chem. 70 (2022) 16229–16240.
- [6] C. Han, Z.Y. Yu, Y. Zhang, Z. Wang, J. Zhao, S.X. Huang, Z. Ma, Z. Wen, C. Liu, W. Xiang, Discovery of Frenolicin B as potential agrochemical fungicide for controlling fusarium head blight on wheat, J. Agric. Food Chem. 69 (2021) 2108–2117.
- [7] C. Bailly, J.P. Hénichart, Advocacy for the medicinal plant Artabotrys hexapetalus (Yingzhao) and antimalarial Yingzhaosu endoperoxides, Molecules 27 (2022) 6102
- [8] Y.H. Lan, H.Y. Wang, C.C. Wu, S.L. Chen, C.L. Chang, F.R. Chang, Y.C. Wu, New constituents from stems of *Artabotrys uncinatus*, Chem. Pharm. Bull. 55 (2007) 1597–1599.
- [9] Q. Zhou, Y.H. Fu, Li Xb, G.Y. Chen, S.Y. Wu, X.P. Song, Y.P. Liu, C.R. Han, Bioactive benzylisoquinoline alkaloids from *Artabotrys hexapetalus*, Phytochem. Lett. 11 (2015) 296–300.
- [10] T.J. Hsieh, C.Y. Chen, R.Y. Kuo, F.R. Chang, Y.C. Wu, Two new alkaloids from Artabotrys uncinatus, J. Nat. Prod. 62 (1999) 1192–1193.
- [11] F.M. Xi, S.G. Ma, Y.B. Liu, L. Li, S.S. Yu, Artaboterpenoids A and B, Bisabolenederived sesquiterpenoids from *Artabotrys hexapetalus*, Org. Lett. 18 (2016) 3374–3377.
- [12] F.M. Xi, Y.B. Liu, J. Qu, Y. Li, Z.H. Tang, L. Li, Y.H. Li, X.G. Chen, S.G. Ma, S.S. Yu, Bioactive sesquiterpenoids from the roots of *Artabotrys hexapetalus*, Tetrahedron 73 (2017) 571–582.
- [13] T.M. Li, W.K. Li, J.G. Yu, Flavonoids from Artabotrys hexapetalus, Phytochemistry 45 (1997) 831–833.
- [14] P. Tomšík, S. Mičuda, D. Muthná, E. Čermáková, R. Havelek, E. Rudolf, M. Hroch, Z. Kadová, M. Rezáčová, J. Ćmielová, P. Živný, Boldine inhibits mouse mammary carcinoma in vivo and human MCF-7 breast cancer cells in vitro, Planta Med. 82 (2016) 1416–1424.
- [15] H.M. Malebo, T. Wenzler, M. Cal, S.M. Swaleh, M.O. Omolo, A. Hassanali, U. Séquin, D. Häussinger, P. Dalsgaard, M. Hamburger, R. Brun, I.O. Ndiege, Antiprotozoal activity of aporphine and protoberberine alkaloids from *Annickia kummeriae* (Engl. & Diels) Setten & Maas (Annonaceae), BMC Complement. Altern. Med. 13 (2013) 48.
- [16] A. Makarasen, W. Sirithana, S. Mogkhuntod, N. Khunnawutmanotham, N. Chimnoi, S. Techasakul, Cytotoxic and antimicrobial activities of aporphine alkaloids isolated from *Stephania venosa* (Blume) Spreng, Planta Med. 77 (2011) 1519–1524.
- [17] C.C. Wu, C.L. Wu, S.L. Huang, H.T. Chang, Antifungal activity of liriodenine from Michelia formosana heartwood against wood-rotting fungi, Wood Sci. Technol. 46 (2011) 737–747.
- [18] I. De-la-Cruz-Chacón, N.Y. López-Fernández, C.A. Riley-Saldaña, M. Castro Moreno, A.R. González-Esquinca, Antifungal activity in vitro of Sapranthus microcarpus (Annonaceae) against phytopathogens, Acta Bot. Mex. 126 (2019) 1–10.
- [19] X.B. Huang, N. Hao, Q. Wang, R.R. Li, G. Zhang, G.Q. Chen, S.M. Liu, Z.P. Che, Non-food bioactive forest product liriodenine: sources, chemistry, and bioactivities, Ind. Crop. Prod. 187 (2022) 115447.
- [20] C.F. Zhang, N. Nakamura, S. Tewtrakul, M. Hattori, Q.S. Sun, Z.T. Wang, T. Fujiwara, Sesquiterpenes and alkaloids from *Lindera chunii* and their inhibitory activities against HIV-1 integrase, Chem. Pharm. Bull. 50 (2002) 1195–1200.
- [21] C.M. Liu, C.L. Kao, H.M. Wu, W.J. Li, C.T. Huang, H.T. Li, C.Y. Chen, Antioxidant and anticancer aporphine alkaloids from the leaves of *Nelumbo nucifera Gaertn. cv. Rosa-plena*, Molecules 19 (2014) 17829–17838.
- [22] N. Santanam, M. Penumetcha, H. Speisky, S. Parthasarathy, A novel alkaloid antioxidant, Boldine and synthetic antioxidant, reduced form of RU486, inhibit the

- oxidation of LDL *in-vitro* and atherosclerosis *in vivo* in LDLR $^{-/-}$ mice, Atherosclerosis 173 (2004) 203–210.
- [23] Z.Z. Zhang, ElSohly HN, M.R. Jacob, D.S. Pasco, L.A. Walker, A.M. Clark, New sesquiterpenoids from the root of *Guatteria multivenia*, J. Nat. Prod. 65 (2002) 856–859.
- [24] M. Fontes Barbosa, A. Benatti Justino, M. Machado Martins, K. Roberta Anacleto Belaz, F. Barbosa Ferreira, R. Junio de Oliveira, A. Danuello, F. Salmen Espindola, M. Pivatto, Cholinesterase inhibitors assessment of aporphine alkaloids from Annona crassiflora and molecular docking studies, Bioorg. Chem. 120 (2022) 105593.
- [25] T.J. Hsieh, F.R. Chang, Y.C. Chia, C.Y. Chen, H.C. Lin, H.F. Chiu, Y.C. Wu, The alkaloids of Artabotrys uncinatus, J. Nat. Prod. 64 (2001) 1157–1161.
- [26] C.Y. Chen, F.R. Chang, C.M. Teng, Y.C. Wu, Cheritamine, a new-fatty acyl tryptamine and other constituents from the stems of *Annona cherimola*, J. Chin. Chem. Soc. 46 (1999) 77–86.
- [27] M.H.H. Nkunya, S.A. Jonker, J.J. Makangara, R. Waibel, H. Achenbach, Aporphinoid alkaloids and other constituents from *Lettowianthus stellatus*, Phytochemistry 53 (2000) 1067–1073.

- [28] H.L.M. Guinaudeau, A. Cavé, Aporphinoid alkaloids, III, J. Nat. Prod. 46 (1983) 761–835.
- [29] H.L.M. Guinaudeau, A. Cavé, Aporphinoid alkaloids, V. J. Nat. Prod. 57 (1994) 1033–1135.
- [30] D.L. Yang, W.L. Mei, H. Wang, H.F. Dai, Antimicrobial alkaloids from the tubers of Stephania succifera, Z. Naturforsch. 65b (2010) 757–761.
- [31] Y.K. Zheng, B.J. Su, Y.Q. Wang, H.S. Wang, H.B. Liao, D. Liang, New tyramine- and aporphine-type alkamides with NO release inhibitory activities from *Piper puberulum*, J. Nat. Prod. 84 (2021) 1316–1325.
- [32] Z. Yu, L. Wang, J. Yang, F. Zhang, Y. Sun, M. Yu, Y. Yan, Y.T. Ma, S.X. Huang, A new antifungal macrolide from *Streptomyces* sp. KIB-H869 and structure revision of halichomycin, Tetrahedron Lett. 57 (2016) 1375–1378.
- [33] V.V. Krishnan, S. Vazquez, K. Maitra, S. Maitra, Restricted amide rotation with steric hindrance induced multiple conformations, Chem. Phys. Lett. 689 (2017) 148–151
- [34] Z.F. Chen, Y.C. Liu, Y. Peng, X. Hong, H.H. Wang, M.M. Zhang, H. Liang, Synthesis, characterization, and in vitro antitumor properties of gold (III) compounds with the traditional Chinese medicine (TCM) active ingredient liriodenine, J. Biol. Inorg. Chem. 17 (2012) 247–261.